



Transition metal salt assisted dilute acid hydrolysis for synthesis of microcrystalline cellulose from *Teff Straw*

Equar Gebre Assefa · Zebene Kiflie ·
Hundessa Dessalegn Demsash

Received: 24 September 2022 / Accepted: 15 May 2023 / Published online: 1 June 2023
© The Author(s), under exclusive licence to Springer Nature B.V. 2023

Abstract The utilization of agricultural residues for value-added products has the potential to contribute to a cleaner environment. The aim of this study was to characterize microcrystalline cellulose (MCC) isolated from *Teff* straw (TS) in a multi-step method that included alkaline treatment, alkaline hydrogen peroxide bleaching, and catalyzed dilute acid hydrolysis. FT-IR, SEM, XRD, and TGA were used to characterize changes in the chemical and physical properties of samples. FT-IR results indicated the removal of non-cellulosic components, while the x-ray diffraction revealed a significant increase in crystallinity during pretreatment and the subsequent catalyzed acid hydrolysis. The crystallinity index (CrI) values for the prepared microcrystalline cellulose (Cr(III), Fe(III)Cl, and Fe(III) catalyzed MCC) were 73.34%, 67.58% and 66.69% respectively. Additionally, from the TGA analysis, the MCC samples showed T_{onset} and T_{max} values of (285, 359), (273, 340), and (275, 335) °C for the Cr(III), Fe(III)Cl, and Fe(III) catalyzed MCC,

respectively. The results imply that $\text{Cr}(\text{NO}_3)_3$ catalyzed dilute acid hydrolysis produces MCC with the highest crystallinity and best thermal stability. Overall, the results of this study showed that TS could be used as a new source to obtain MCC. Furthermore, the preparation method used in this study could also be a preferential method over the conventional mineral acid hydrolysis.

Keywords *Teff straw* · Pretreatment · MCC isolation · Characterization

Introduction

Microcrystalline cellulose (MCC) is a white, fine, odorless, and crystalline powder obtained through the depolymerisation of the amorphous region of cellulose (Asif et al. 2022). The isolation of MCC from various sources has gained interest due to its unique physicochemical properties, such as small particle sizes, renewability, excellent mechanical properties, large surface area, and biocompatibility (Gichuki et al. 2022). These important characteristics make microcrystalline cellulose a very promising material as a bio-filler for polymer composite materials. Recent scientific and technological research has focused on the utilization of agricultural residues for the extraction of MCC because of their low—cost, naturally abundance, and renewability. Agricultural residues such as cotton stalk waste (Li et al. 2019),

E. G. Assefa · Z. Kiflie (✉)
School of Chemical and Bioengineering, Addis Ababa
Institute of Technology, Addis Ababa University,
Addis Ababa, Ethiopia
e-mail: kifliez@gmail.com; zebene.kiflie@aau.edu.et

E. G. Assefa
e-mail: enquegeb@gmail.com

H. D. Demsash
Chemical Industries Corporation, Addis Ababa, Ethiopia
e-mail: hundessad@gmail.com

tea waste (Zhao et al. 2018), sugarcane bagasse (Katakajwala and Mohan 2020), rice husk (Ohwoav-worhwa et al. 2019), were previously exploited for the preparation of microcrystalline cellulose.

Teff is the main cultivated cereal crop in Ethiopia which is used as the major staple food. As a result, a lot of *Teff* straw (TS) is generated each year throughout the country. *Teff* straw is mainly used for animal feeding and is often disposed of as waste. As reported in our previous work, TS has a chemical composition of approximately 40 wt.%, 29 wt.%, and 18 wt.% of cellulose, hemicellulose, and lignin, respectively (Assefa et al. 2022), showing higher cellulose content than those of corn stover (36.5), rice straw (32), wheat straw (29–35), and banana waste (13.2) (Kapoor et al. 2016; Yang et al. 2016), and lower than sugarcane bagasse fibers (45) (Borges et al. 2016). Thus, TS could be exploited as a viable alternative cellulosic material for microcrystalline cellulose production.

The preparation of MCC from cellulose is mainly performed through acid hydrolysis (Trache et al. 2016). It produces MCC with high crystallinity index as the amorphous phase of cellulose is readily hydrolyzed when exposed to the mineral acid. Many previous studies indicate that concentrated mineral acids have been used for the extraction of MCC from various biomass sources. Hachaichi et al. (2021) extracted MCC from Palm Fibers using 64 wt.% of sulphuric acid (H_2SO_4) solution at 45 °C for 30 min. Asif et al. (2022) also isolated MCC from *Lagenaria siceraria* fruit pedicles with 40% H_2SO_4 at 95 °C for 40–50 min. The acid hydrolysis method is a simple and rapid process for microcrystalline cellulose production; nevertheless, the procedure is normally associated with several restrictions, such as corrosion of equipment, the need for a large amount of water, the difficulty of acid recovery, and over-degradation of cellulose. In some cases, researchers have used a combination of acid hydrolysis with other methods to increase the fibrillation of cellulose. Ismail et al. (2021) prepared MCC using steam-assisted acid hydrolysis from palm empty fruit bunch fiber.

Transition metal salt catalysts have been widely and effectively employed in various types of chemical reactions. They are Lewis acids and have received use as acid homogenous catalysts for the cellulose hydrolysis. It had been proved that the metal ion catalyst was capable to accelerate the cellulose hydrolysis and enhance the catalytic activity by reducing the

activation energy of the hydrolysis reaction (Zhang et al. 2015). Additionally, the metal salts render high hydrolysis selectivity, which favors targeting the C–O–C and C–H bonds of cellulose in lignocellulosic biomass polymer networks (Wei et al. 2011). Furthermore, the metal salts are less corrosive, show less severity conditions, and can be recovered through ultrafiltration process as compared to the strong mineral acids.

Based on literature studies, Iron and chrome-based catalysts were found to contain Lewis acid sites and can perform the hydrolysis of cellulose efficiently. Lu's group has prepared nanocellulose through ultrasonication-assisted $FeCl_3$ -catalyzed hydrolysis from bamboo pulp (Lu et al. 2014). Their research findings indicate that Fe^{3+} can selectively diffuse into the amorphous regions of cellulose and promote the cleavage of glycosidic linkages of cellulose chains into smaller dimensions. Chromium-based metal salt catalysts have also been highly effective in breakage of glycosidic linkage and hydrogen bonding within the cellulose matrix (Chen et al. 2016b, 2017a, b). Furthermore, the valence state of the transition metal ion plays a significant role in hydrolysis efficiency (Kamireddy et al. 2013). A higher valence state will generate more H^+ ions, which act effectively in the co-catalyzed acid hydrolysis reaction in the presence of metal ions. Chen's research group studied the effect of $Fe(NO_3)_3$, $Co(NO_3)_2$ and $Ni(NO_3)_2$ -metal salts, and the results showed that crystallinity index of the prepared nanocellulose hydrolyzed with the trivalent Fe^{3+} catalyst was higher than cellulose treated by the divalent Co^{2+} and Ni^{2+} catalyst under same hydrolysis condition (Chen et al. 2016a). Hence in this study, Iron and chrome-based metal salt with trivalent ions (Chromium (III) nitrate [$Cr(NO_3)_3$], Iron (III) chloride [$FeCl_3$], and Iron (III) nitrate [$Fe(NO_3)_3$]) were selected as catalysts to depolymerize a pretreated *Teff* straw fiber into microcrystalline cellulose.

On the other hand, during sulphuric acid hydrolysis, negative surface charges are generated on the surface hydroxyl groups of cellulose crystals which provide more stable suspensions. Hence, the presence of the acidic medium (H_2SO_4) could have a synergistic effect during the transition metal ions-catalyzed acid hydrolysis process.

Because of its less familiarity in the scientific community, only very few Ethiopian scholars have tried to investigate the use of TS for biogas production

(Chufu et al. 2015), bio silica synthesis (Bageru and Srivastava 2017; Wassie and Srivastava 2017), and as adsorbent for chrome removal (Wassie and Srivastava 2016). Since *Teff* is cultivated on a large scale in Ethiopia, the successful preparation of MCC from this plentiful source could provide valuable crystalline cellulose material with the possibility to be used as green filler in bio-composite applications. To date, no published studies have been reported on the preparation of microcrystalline cellulose from TS by acid hydrolysis with transition metal salt catalysts.

Thus, the objectives of this study were to isolate and characterize MCC from *Teff* straw via transition metal salts catalyzed dilute acid hydrolysis. The effects of three trivalent transition metals salts, Chromium (III) nitrate [$\text{Cr}(\text{NO}_3)_3$], Iron (III) chloride [FeCl_3], and Iron (III) nitrate [$\text{Fe}(\text{NO}_3)_3$] used as catalysts were investigated. Furthermore, changes in crystallinity, morphology, particle size and thermal properties of the obtained MCC were studied.

Materials and methods

Materials

The chemical reagents used were Sulfuric acid (H_2SO_4 , 98% purity), Sodium hydroxide, Hydrogen peroxide (H_2O_2 , 30%), Glacial acetic acid, Nitric acid (HNO_3 , 69%), Perchloric acid (HClO_4 , 70%), Ethanol, Chromium (III) nitrate ($\text{Cr}(\text{NO}_3)_3$), Iron(III) chloride (FeCl_3), and Iron (III) nitrate ($\text{Fe}(\text{NO}_3)_3$). All chemical reagents were of analytical grades.

Methods

Pretreatment

The pretreatment of TS was conducted mainly through a three-step process—namely hot water, alkali, and bleaching treatments, as described elsewhere (Assefa et al. 2022). Firstly, TS was collected from a local farm, cleaned thoroughly, sun-dried for 72 h, and milled. It was then boiled in distilled water (liquor ratio of 1:50 g/mL) at 70 °C for 2 h under constant stirring. The sample thus treated was filtered and washed with cold distilled water to remove water-soluble extractives, and left overnight for drying in a

hot air oven at 60 °C. This sample was labeled as hot water-treated TS and stored in an airtight plastic bag to prevent fungal development.

The hot water-treated TS (5 g) was then treated with 150 mL of sodium hydroxide solution (5 wt.%) at 90 °C for 1.5 h under strong stirring to remove lignin and hemicellulose from TS. The resulting sample was cooled to room temperature and filtered to separate the liquid fraction from the solid one. After filtration, the solid residue was washed with distilled water and oven dried at 60 °C. Subsequently, bleaching treatment was done by adding the obtained alkali treated and dried fiber in a preheated mixture of H_2O_2 (20 wt.%) and NaOH (5 wt.%) at 65 °C under continuous stirring for 1.5 h. At the end of the reaction, the sample was filtered and washed with distilled water several times until the pH became neutral. This bleaching treatment was repeated two times. Finally, the residue was dried in an oven at 60 °C until a constant weight was reached and pulverized into powder resulting in pure white colored cellulose fibers. In these alkali and bleaching treatments, the fibers to liquor ratios were kept at 1:30 (g/mL).

Synthesis of microcrystalline cellulose (MCC) by metal salts assisted dilute acid hydrolysis

Cellulose microcrystals were prepared from the pretreated TS fiber by three transition metal salt catalysts assisted dilute acid hydrolysis process. 15% sulfuric acid and 0.6 M of each catalyst ($\text{Cr}(\text{NO}_3)_3$, FeCl_3 , and $\text{Fe}(\text{NO}_3)_3$) were mixed separately at a ratio of 1:1 (v/v), to obtain three types of dilute acid solutions. Then, 5 g of pretreated TS sample was added to the prepared mixed acid solution at solid cellulose to liquor ratio of 1:40 g/mL. The hydrolysis was performed in an atlas reactor at 60 °C for 1.5 h to hydrolyze the amorphous domains of the obtained cellulose fibers. Following the completion of the hydrolysis, the suspension was diluted with excess cold distilled water to stop the reaction. This suspension was then filtered and washed using distilled water repeatedly until neutral pH was achieved. Finally, the sample was dried at 50 °C in a vacuum oven to constant weight and pulverized to powder using a high-speed universal disintegrator (FW100, China). Figure 1 shows the process flow diagram for the isolation of microcrystalline cellulose from TS. The raw, pretreated

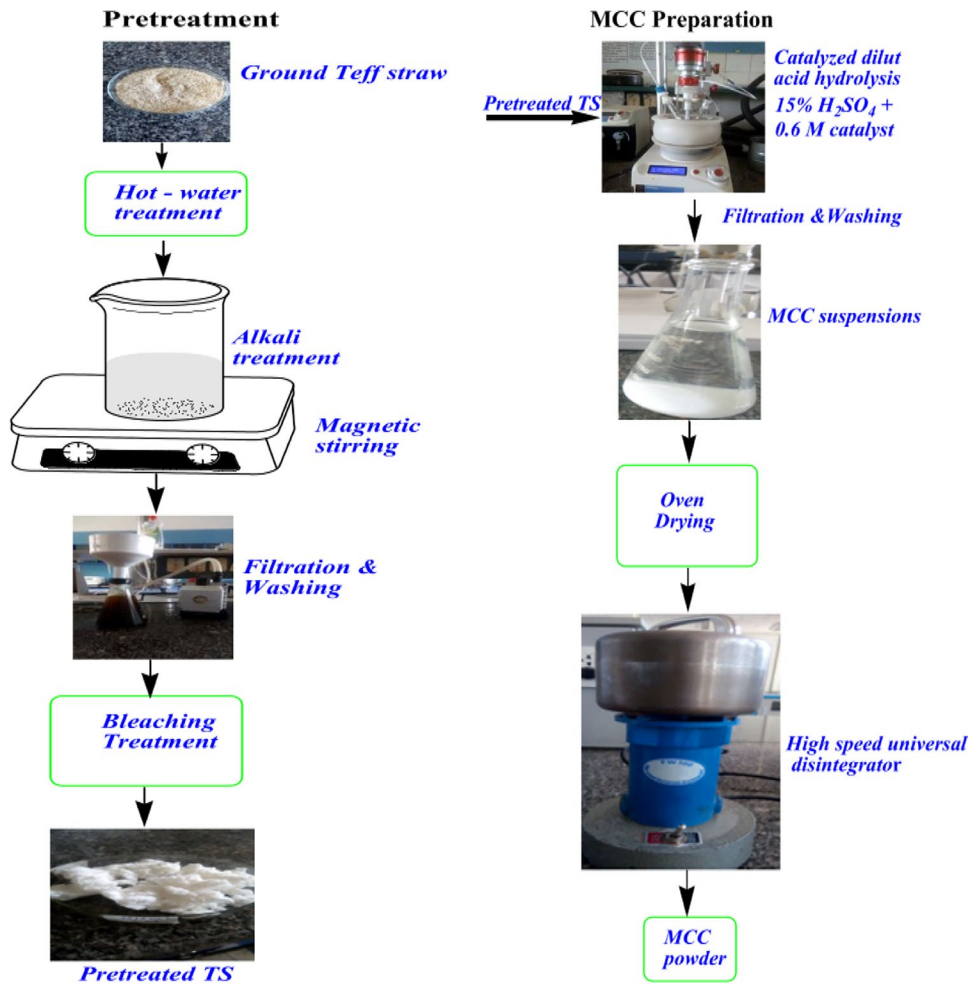


Fig. 1 Schematic representation for the isolation of MCC fiber from TS via catalyzed dilute acid hydrolysis

and the obtained products are labeled as Raw—TS, Pretreated—TS, Cr (III)—MCC, Fe(III)Cl—MCC, and Fe(III)—MCC, respectively where the obtained MCC are labeled depending on the type of catalyst used during the extraction.

The yield (%) of microcrystalline cellulose was estimated gravimetrically based on its dry weight before and after the MCC synthesis according to Eq. (1) below:

$$\text{yield}_{\text{MCCs}}(\%) = \frac{M_{\text{MCCs}}}{M_{\text{Pretreated TS}}} \times 100 \quad (1)$$

where M_{MCC} is the dry mass of the obtained microcrystalline cellulose, and $M_{\text{Pretreated TS}}$ is the dry mass of the pre-treated *Teff* straw residue.

Biomass Composition Analysis

The detail of the chemical composition determination of the raw and pretreated *Teff* straw fiber was presented in the previous work (Assefa et al. 2022). The amount of extractives was calculated by water/alcohol extraction method using the NREL/TP-510-42,619 method (Sluiter et al. 2008b). Whereas, inorganic material (ash) content was determined by placing a measured sample in a muffle furnace at 575 °C based

on the NREL/TP-510-42,622 procedure (Sluiter et al. 2008a). For lignin content determination, a two-step acid hydrolysis based on NREL/TP-510-42,618, method was used (Sluiter et al. 2004). Similarly, cellulose content was determined by hydrolyzing with a mixture of nitric acid and ethanol according to the Kurschner-Hoffer gravimetric method (Kürschner 1931). Finally, the hemicellulose content of TS (%w/w) was calculated by difference assuming that extractives, hemicellulose, lignin, cellulose, and ash are the only components of the entire biomass.

Microcrystalline cellulose characterization

Functional groups present in the samples were examined using FT-IR (JASCO FT/IR-6600) in the wave number range 500–4000 cm^{-1} with a resolution of 4 cm^{-1} . The x-ray diffraction (XRD) profiles of the different samples were obtained using an x-ray diffractometer (D2 phaser, Bruker, Germany) with $\text{CuK}\alpha$ radiation ($\lambda=0.15406$ nm), and operated at 30 kV and 10 mA. Samples were scanned at ambient condition in the 2θ range of 10° – 40° at a scanning rate of $1^\circ/\text{min}$. The crystallinity index (CrI) was calculated according to the method described by Segal et al. (1959).

$$\text{CrI}(\%) = \frac{I_{200} - I_{\text{am}}}{I_{200}} \times 100 \quad (2)$$

where *CrI* is the relative degree of crystallinity, I_{200} represents to the highest peak intensity at the lattice diffraction (200) of the crystalline regions and I_{am} is the minimum value between planar reflections (200) and (110), which refers to reflection intensity of the amorphous parts of the samples.

The mean crystallite size (*D*) of the microcrystalline cellulose fibers was estimated using Scherer equation (Kumar et al. 2014).

$$D = \frac{\kappa \lambda}{\beta \cos \theta} \quad (3)$$

where κ is a Scherrer constant (0.89), λ is the x-ray wavelength of the radiation which is constant ($\lambda=0.15406$ nm), β = full width at half-max of the XRD peak, and θ is diffraction angle in radians.

Thermogravimetric analysis of the raw TS, pre-treated TS fiber, and the microcrystalline cellulose prepared by three different catalysts was performed

using a thermal analyzer (HCT-1, BJHENVEN, China) to determine the thermal decomposition of fibers in the temperature range of 20–700 $^\circ\text{C}$ at a constant heating rate of 20 $^\circ\text{C}/\text{min}$ under a nitrogen environment. The surface morphologies were analyzed using a field emission scanning electron microscope (JEOL JSM-IT 100, Japan).

The AAS used for the analysis of the metals was PG Instruments (AA500 spectrophotometer, England) equipped with deuterium lamps and hollow cathode lamps with air-acetylene flame. The wavelength was set at 357.9 and 248.3 nm for chrome (Cr (III)) and iron (Fe(III)) concentration determination, respectively. Such technique of elemental analysis requires aqueous samples. Thus, solid samples were converted into solutions. Nitric–perchloric acid sample digestion method was used for the dissolution of MCC samples as described elsewhere (Uddin et al. 2016). Briefly, 0.5 g of samples were weighed and mixed with 5 ml of concentrated HNO_3 in a 125 ml Erlenmeyer flask. The mixture was boiled on a hot plate for 40 min. After cooling, 2.5 ml of 70% HClO_4 was added and the mixture was boiled until dense white fumes appeared. After cooling and filtration, the solution was transferred quantitatively into a 50 mL volumetric flask for analysis.

Results and Discussion

Chemical compositions analysis

In a previous study (Assefa et al. 2022), we determined the chemical compositions of the raw TS and the results showed that the raw fibers contained 40% cellulose, 29% hemicellulose, and 18 wt.% lignin. However, the chemical composition of raw TS was changed after the chemical treatments. The cellulose content increased from 40 to 68.5 wt.% while, hemicellulose and lignin contents were reduced to 21 and 7 wt.%, respectively after the alkali treatment. The significant decrease in lignin content from the raw TS was due to the disruption and breaking of hydrogen bonds through NaOH treatments. To further eliminate the residual lignin, the NaOH-treated samples were subjected to a hydrogen peroxide treatment at alkaline conditions where the cellulose content was further increased to 85.5 wt.% with lignin and hemicellulose

contents of 2.5 and 12 wt.%, respectively. Furthermore, the obtained pretreated fiber was pure white suggesting the removal of most of the non-cellulosic components from the TS (Fig. 1).

FTIR analysis

Figure 2 presents the FTIR spectra of the raw TS, pretreated fibers, and microcrystalline cellulose isolated by catalyzed diluted acid hydrolysis. The figure clearly shows that all samples exhibit similar peaks at 3410, 2900, 1430, 1382, and 890 cm^{-1} which are related to the cellulose I characteristic absorption peaks. As reported elsewhere (Le Troedec et al. 2008), the peak at around 3400 cm^{-1} is characteristic of the O–H stretching intermolecular hydrogen bonds; while the peak at 2900 cm^{-1} corresponds to the C–H symmetrical stretching group present in the carbohydrates of cellulose. Likewise, the typical spectral bands observed at 1430, and 897 cm^{-1} are attributed to the symmetric bending of CH_2 and β -glycosidic linkages between glucose units of cellulose, respectively. In addition, the vibration peak detected at 1382 cm^{-1} in all samples has been associated with the C–H bending in the cellulose. Furthermore, a peak at around 1644 cm^{-1} which is attributed to the O–H bending due to water adsorbed in the fibers is observed in all samples. The fact that the cellulose I characteristic peaks remain in the MCC indicates that the pretreatment and the hydrolysis processes have not changed the main chemical structure of cellulose (French 2014).

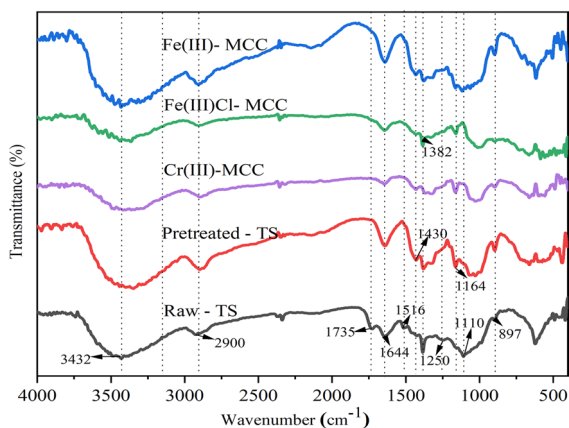


Fig. 2 FTIR spectrum of (a) *Teff* Straw as raw material, (b) chemically purified cellulose and (c) the obtained MCC

However, in the FTIR spectra of the raw TS fiber, there appear some peaks that are not observed in the spectra of the pretreated fiber and synthesized MCC. These include the peaks at 1730 cm^{-1} which correspond to C–O stretching vibration for the acetyl and ester linkages in lignin and hemicellulose, and the peaks at 1502 and 1250 cm^{-1} which are attributed to the C=C stretching vibrations of the aromatic rings and C–O out-of-plane stretching due to the aryl group in lignin, respectively (Zhang et al. 2020). Presumably, the disappearance of these absorption peaks in the FTIR spectra of pretreated fiber and synthesized MCC are related to the successful removal of lignin and hemicellulose as a result of the pretreatment and catalyzed dilute acid hydrolysis processes. This observation is in agreement with similar investigations reported in the literature (Feng et al. 2020). Furthermore, a peak at 1110 cm^{-1} , which is associated with the C–O–C stretching of hemicellulose, is observed in the FTIR spectra of the raw TS indicating the presence of hemicellulose. However, this peak gradually disappeared in the isolated MCC spectra, suggesting that hemicellulose was successfully removed because of hydrolysis. On the contrary, the peaks at 1164 and 897 cm^{-1} which are associated with the C–O–C stretching of cellulose and C–H deformation of glycosidic linkages between glucose units in cellulose (Zhuang et al. 2020), have increased in intensity after the pretreatment and catalyzed dilute acid hydrolysis of TS.

Overall, the obtained FTIR spectra of the samples are in agreement with those where similar findings were reported in the literature for other lignocellulose.

Thermogravimetry analysis (TGA)

The determination of thermal stability of microcrystalline cellulose is a key factor for its potential use as a reinforcing agent in bio-composites. The thermal degradation characteristics of the untreated TS, pretreated fiber and the prepared microcrystals are presented in Fig. 3. The degradation onset temperature (T_{onset}), the maximum degradation temperature (T_{max}), and the maximum weight loss (WL_{max}) for raw, pretreated TS, and obtained MCC are summarized in Table 1.

Figure 3 shows an initial small mass loss in the temperature range of 40–110 $^{\circ}\text{C}$ which may be due to the evaporation and removal of bound water and loss

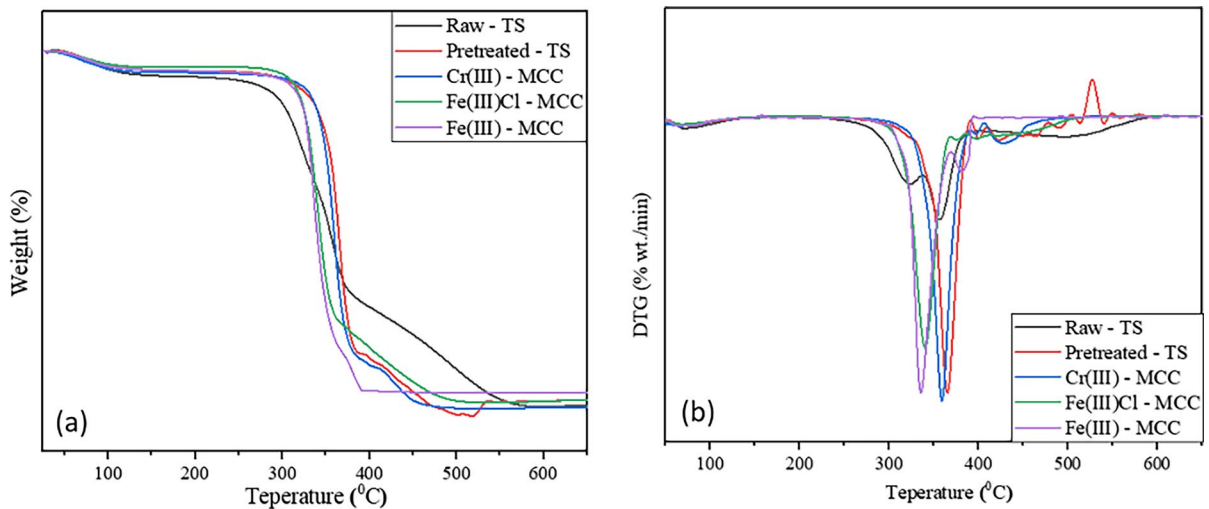


Fig. 3 TGA and DTG curves of Raw TS fibers, Pretreated TS fiber and the prepared MCC

Table 1 Onset temperature (T_{onset}), maximum decomposition temperature (T_{max}), and corresponding percentage of weight losses of the raw, pretreated fiber, and obtained MCC

| Sample | Code | First thermal degradation range | WL (%) | T_{onset} (°C) | DTG T_{max} (°C) | WL $_{\text{max}}$ (%) |
|---|---------------|---------------------------------|--------|-------------------------|---------------------------|------------------------|
| Raw fiber | Raw-TS | 45–110 | 5.8 | 230 | 356 | 46.1 |
| Pretreated TS | Pretreated-TS | 60–120 | 4.8 | 255 | 365.5 | 65.1 |
| Cr(NO ₃) ₃ treated | Cr(III)-MCC | 56–106 | 5.01 | 285 | 359 | 73.52 |
| FeCl ₃ treated | Fe(III)Cl-MCC | 50–110 | 3.89 | 273 | 340 | 67.45 |
| Fe(NO ₃) ₃ treated | Fe(III)-MCC | 56–107 | 4.76 | 275 | 335 | 72.27 |

of extractives existing in the fibers. This is in agreement with the FTIR analyses results which indicate the presence of absorbed water in the fibers. Furthermore, comparing the weight loss in this region among the different samples, the MCC generally shows smaller weight loss as compared to the raw TS. This finding implies that the moisture content of MCC was slightly lower than those of raw TS fiber which may be due to the introduction of sulfate groups at the outer surface of MCC during the acid hydrolysis process. The second degradation occurs in the temperature range of 250–320 °C, resulting mainly from the thermal decomposition of hemicellulose and some portion of lignin. The presence of acetyl groups might have made hemicellulose more susceptible to thermal degradation than cellulose. The thermal decomposition peak for hemicellulose which is shown on

the DTG graph of the raw TS has disappeared, as expected, in the prepared MCC.

The final major decomposition range is observed in the high temperature range (300–390 °C) which is related to the cellulose degradation due to the depolymerization of glycosyl units. From the TGA analysis, the T_{onset} values of TS, Cr(III)-MCC, Fe(III)Cl-MCC, and Fe(III)-MCC were 230, 285, 273, and 275 °C, respectively (Table 1). The observed increase in the T_{onset} of MCC might be a result of the removal of hemicellulose and lignin components which were present in the raw TS. The hemicellulose and lignin components had low thermal degradation temperatures, and the degradation of one of these components could initiate the thermal degradation of the surrounding cellulose fibers (Tian et al. 2017). The higher T_{onset} values of the MCC indicate the higher thermal stability of these fibers. However, it is worth

to note that the Cr (NO₃)₃ catalyzed and extracted MCC has exhibited the highest T_{onset} value of 285 °C, which is 55 °C higher than that of the raw TS.

Furthermore, in the same high temperature degradation range, differences in maximum degradation temperatures (T_{max}) are observed among the different samples. In this regard, the pretreated cellulose fiber shows a higher degradation temperature than the MCC (Table 1). This might be related to the smaller particle sizes of the MCC (increase in specific surface area) which have facilitated the thermal degradation to occur at lower temperatures (Cheng et al. 2014; Maiti et al. 2015). Fe (NO₃)₃—treated microcrystalline cellulose exhibited the lowest T_{max} value of 335.0 °C, which was 21.0 °C lower than that of raw TS.

Overall, the higher thermal stability (higher T_{onset} and T_{max} values) of the isolated MCC could be attributed to the higher crystallinity of the obtained MCC as well as to the removal of hemicellulose and lignin from these fibers (Panthapulakkal et al. 2006; Alemadar and Sain 2008). These results are very consistent with the results obtained from XRD and FTIR analysis results. Therefore, from the TGA, it can be concluded that MCC prepared from TS by using transmission metal salts assisted dilute sulfuric acid hydrolysis exhibit higher thermal stability. This is an important factor for the use of the prepared MCC in various industrial applications, especially in the thermoplastics field, as the processing temperature is normally higher than 200 °C (Cheng et al. 2014).

X-ray diffraction analyses (XRD)

Cellulose has a crystalline structure in nature owing to the hydrogen bonding and Van der Waals forces which strongly hold together its adjacent molecules (Zhang and Lynd 2004). This property makes it different from other components in the lignocellulosic biomass. Moreover, the crystallinity of the extracted microcrystalline cellulose has a direct influence on the strength of biocomposite materials with MCC as fillers (Ahvenainen et al. 2016). However, since the crystallinity and the size of the crystallites of MCC could be affected during the MCC isolation processes, x-ray Diffraction analyses were conducted to study the crystalline behavior of the three MCC obtained from TS.

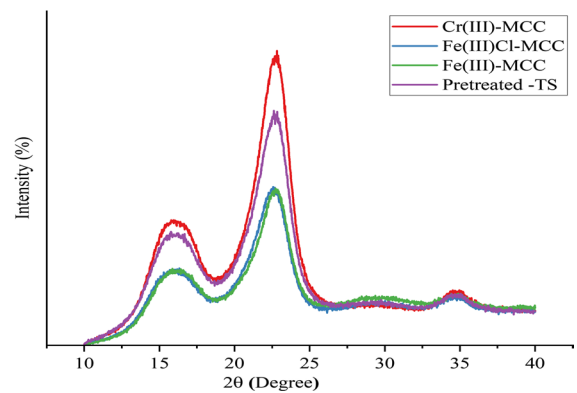


Fig. 4 XRD diffraction patterns of pretreated TS fibers, and the prepared microcrystalline cellulose

Figure 4 gives the XRD patterns of the studied samples. The XRD patterns in this figure reveal that all samples exhibit the three distinct peaks of cellulose at 2θ values of 16.3°, 22.4°, and 34.5°, confirming that the cellulose-I allomorph is well-maintained after the dilute acid hydrolysis process (Sun et al. 2015; Zhuang et al. 2020).

Further information can also be obtained from the CrI and the average crystallite sizes summarized in Table 2. As can be observed from this table, all treated samples (PTS, Cr(III)-MCC, Fe(III)Cl-MCC and Fe(III)-MCC) show significant increases in the CrI values with respect to raw TS. Since CrI is a parameter that quantifies the relative amount of crystalline material present in a sample, the findings imply that relative amount of crystalline material has increased in the MCC. Similar findings have been reported elsewhere (Feng et al. 2020). Table 2 also shows that the MCC has larger crystallite sizes as compared to the raw TS.

This was mainly due to the removal of lignin and hemicellulose, alignment of the crystalline domains into more ordered conformation, and subsequent release of individual crystallites in the MCC samples (Chen et al. 2016b, 2017a). Among the prepared microcrystalline cellulose, Cr (III)-MCC sample shows higher crystallinity (Table 2) as compared to Fe (III)Cl-MCC and Fe(III)-MCC samples which suggests Cr (III) ion was more effective for selective hydrolysis of the amorphous phase of the fiber. In addition to the CrI, the crystallite size is also supportive for the description of crystallinity of the yielded microcrystalline cellulose. From Table 2, the

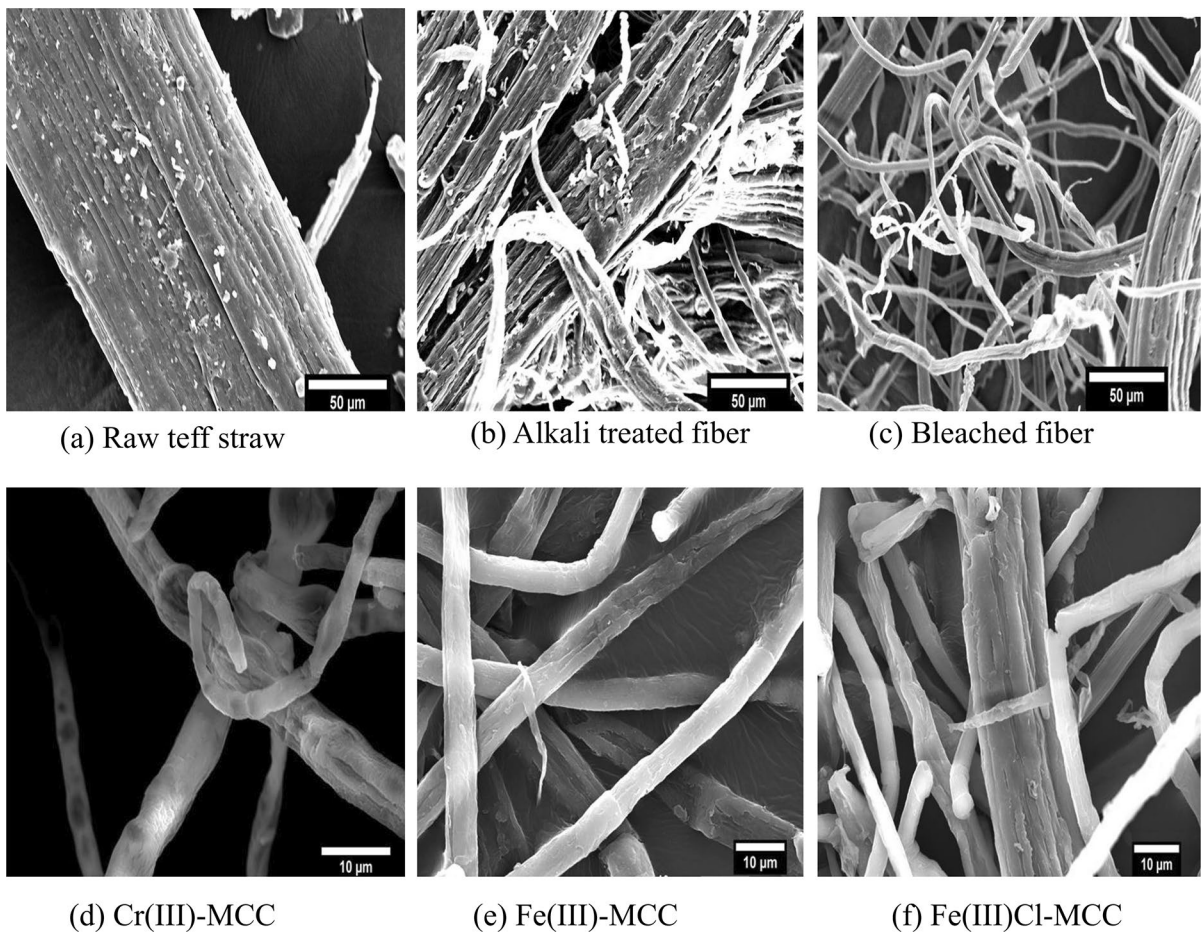
Table 2 Crystallinity index values and Crystallite size of raw TS, pretreated TS fiber, and obtained MCC

| Sample | Code | Yield (%) | Crystallinity index | Crystallite size (D = nm) |
|---|---------------|-----------|---------------------|---------------------------|
| Raw TS | Raw-TS | – | 50.58 | 1.03 |
| Pretreated TS | Pretreated—TS | – | 65.51 | 2.99 |
| Cr(NO ₃) ₃ treated | Cr(III)—MCC | 84 | 73.69 | 3.14 |
| FeCl ₃ treated | Fe(III)Cl-MCC | 82 | 67.58 | 2.72 |
| Fe(NO ₃) ₃ treated | Fe(III)-MCC | 76 | 66.69 | 2.83 |

crystal size of the isolated microcrystalline cellulose, Cr(III)–MCC, Fe(III)Cl–MCC, and Fe(III)–MCC calculated by Scherer equation (Eq. 3) was found to be 3.14 nm, 2.72 nm, and 2.83 nm, respectively. Similar results were reported in the literature for MCC isolated from coconut husk fiber and rice husk (An et al. 2020).

Morphological Investigation

Figure 5 shows SEM micrographs of the raw ground TS (a), the alkali treated fiber (b), the pretreated fiber after the removal of lignin and hemicellulose (c) and finally, the microcrystalline cellulose produced by transition metal salts catalyzed dilute acid hydrolysis

**Fig. 5** SEM images of the Raw TS fibers, pretreated TS fibers, and prepared microcrystalline cellulose

of the pretreated fiber (d, e, and f). Based on the SEM results, the obtained images show significant differences in shape and size before and after treatment. The morphology of the raw TS fiber (Fig. 5a) had a regularly arranged, homogenous structure, and bound closely together because of the binding materials around the cellulose fibrils such as hemicellulose, lignin, and other non-cellulosic components which help in the formation of compact structure (Feng et al. 2018). Furthermore, From Fig. 5a it can be seen that the overall surface of raw TS fiber exhibited a smooth surface due to the presence of waxes and oil. After subsequent alkali and bleaching treatments, defibrillation of the raw TS fibers occurred whereby the diameter of the fibrils got reduced to a great extent because of the removal of the binding materials. Thus, the bleaching process makes it suitable for the subsequent acid hydrolysis process to produce MCC. Additionally, as can be observed in Fig. 5c, the resulting pretreated fiber was long in length. This is because in nature each cellulose fiber is made up of several to hundreds of microfibrils that appeared to be assembled together. With further acid hydrolysis treatment, the transition metal, and the hydronium ions generated during the hydrolysis had broken down the fibers into smaller pieces and further reduction of its diameter. Figures 5d, e, and f shows a SEM image of the MCC fibers (Cr (III)–MCC, Fe (III)–MCC, and Fe(III)Cl–MCC), respectively. Additionally, the average diameter for TS, and microcrystalline cellulose (Cr (III)–MCC, Fe (III)–MCC, and Fe(III)Cl–MCC) measured using the ImageJ software was 135.7 μm , 3.67 μm , 5.08 μm , and 4.97 μm , respectively proving that the average diameter of fibers was tremendously reduced throughout the chemical processes.

Atomic absorption spectrometer (AAS) analysis

Atomic absorption spectroscopy (AAS) analysis was applied to investigate the presence of chrome (Cr (III)) and iron (Fe (III)) ions in the prepared MCC. Before the determination of chromium and iron in the real sample, four series of standard chromium and iron solutions in different concentrations were prepared. After determining the absorbance for all the standard solutions, a calibration curve was constructed. The absorbance of the prepared samples was then compared against the calibration to obtain the corresponding concentrations. The levels of metal

Table 3 elemental chemical analysis

| Samples | Code | Metal ion | Concentration (ppm) |
|---|---------------|-----------|---------------------|
| Cr(NO ₃) ₃ treated | Cr(III)—MCC | Cr(III) | 0.348 |
| FeCl ₃ treated | Fe(III)Cl—MCC | Fe(III) | 1.144 |
| Fe(NO ₃) ₃ treated | Fe(III)—MCC | Fe(III) | 0.865 |

ions in each MCC samples were presented in Table 3 below.

The prepared MCC is intended to use as a bio-filler in bio-composite preparation which could be used in the packaging applications. European Union(EU) and United States(USA) sets out a maximum limit of 100 ppm for heavy metals or their compounds in packaging or a packaging component (Report 2011; Conti 2018). This implies that the results of this study (Table 3) were much lower than the maximum permissible limit set by the EU and USA. Thus, it can be concluded that the obtained MCC had been washed efficiently after the hydrolysis process and metal ion was mostly removed from the prepared samples.

Conclusions

Microcrystalline cellulose was successfully prepared from an abundant and low-cost Ethiopian *Teff* straw via alkali and bleaching pretreatments followed by transition metal salts catalyzed dilute acid hydrolysis. Each transition metal catalyst showed different effects on the crystallinity, crystallite size, surface morphology, and thermal stability of the obtained microcrystalline cellulose. Microscopic observation showed the effects of chemical treatments on the surface of the *Teff* straw. The XRD and TGA analyses respectively showed that the MCC has higher crystallinity and thermal stability, respectively. Among the prepared MCC, the Cr(III) ions synthesized MCC rendered relatively the highest crystallinity and thermal stability, reflecting its better hydrolysis selectivity as compared to Fe(III)Cl and Fe(III)-metal ions. Furthermore, all MCC exhibited degradation temperatures higher than typical processing temperatures of polymeric materials, making them suitable for the preparation of polymer-based bio-composite materials. Thus, it

can be said that the method followed in this work has been successful in extracting MCC from TS and the obtained MCC can be used as green and sustainable fillers in bio-composite materials preparation.

Acknowledgments The authors are grateful to the Addis Ababa Institute of Technology, Addis Ababa University, and the Faculty of Chemical and Food Engineering, Bahir Dar University, for providing the necessary support and laboratory facility during conducting this study.

Authors' contributions Mr. Equar G. and Dr. Hundessa D. conceived the original idea. Sample preparation, experiments, and data analysis were performed by Mr. Equar G. Prof. Zebene Kiflie supervised the study. Mr. Equar G. wrote the draft manuscript. Prof. Zebene Kiflie helped shape the research, provided critical feedback, and edited the manuscript. All authors reviewed the results and approved the final version of the manuscript.

Funding The authors declare that no funds, grants, or other support were received to assist with the preparation of this manuscript.

Data availability Data and materials will be made available on request.

Declarations

Conflict of interest The authors declare that they have no competing interests.

Ethics approval Not applicable.

Consent for publication Not applicable.

References

- Ahvenainen P, Kontro I, Svedström K (2016) Comparison of sample crystallinity determination methods by x-ray diffraction for challenging cellulose I materials. *Cellulose* 23:1073–1086. <https://doi.org/10.1007/s10570-016-0881-6>
- Alemdar A, Sain M (2008) Isolation and characterization of nanofibers from agricultural residues—Wheat straw and soy hulls. *BioResource Technol* 99:1664–1671. <https://doi.org/10.1016/j.biortech.2007.04.029>
- An VN, Thuc H, Nhan C et al (2020) Extraction of high crystalline nanocellulose from biorenewable sources of Vietnamese agricultural wastes. *J Polym Environ*. <https://doi.org/10.1007/s10924-020-01695-x>
- Asif M, Ahmed D, Ahmad N et al (2022) Extraction and characterization of microcrystalline cellulose from *Lagenaria siceraria* fruit pedicles. *Polymers (basel)* 14:1–11. <https://doi.org/10.3390/polym14091867>
- Assefa EG, Kiflie Z, Demsash HD (2022) Valorization of abundantly available ethiopian teff (*eragrostis tef*) straw for the isolation of cellulose fibrils by alkaline hydrogen peroxide treatment method. *J Polym Environ*. <https://doi.org/10.1007/s10924-022-02646-4>
- Bageru AB, Srivastava VC (2017) Preparation and characterization of biosilica from teff (*eragrostis tef*) straw by thermal method. *Mater Lett* 206:13–17. <https://doi.org/10.1016/j.matlet.2017.06.100>
- Borges F, Oliveira D, Bras J et al (2016) Production of cellulose nanocrystals from sugarcane bagasse fibers and pith. *Ind Crop Prod* 93:48–57. <https://doi.org/10.1016/j.indcrop.2016.04.064>
- Chen YW, Lee HV, Abd Hamid SB (2016a) Preparation and characterization of cellulose crystallites via Fe(III)-, Co(II)- and Ni(II)-assisted dilute sulfuric acid catalyzed hydrolysis process. *J Nano Res* 41:96–109
- Chen YW, Lee HV, Hamid SBA (2016) Preparation of nanostructured cellulose via Cr(III)- and Mn(II)-transition metal salt catalyzed acid hydrolysis approach. *BioResources* 11:7224–7241. <https://doi.org/10.15376/biores.11.3.7224-7241>
- Chen YW, Lee HV, Abd Hamid SB (2017a) Investigation of optimal conditions for production of highly crystalline nanocellulose with increased yield via novel Cr(III)-catalyzed hydrolysis: response surface methodology. *Carbohydr Polym* 178:57–68. <https://doi.org/10.1016/j.carbpol.2017.09.029>
- Chen YW, Tan TH, Lee HV, Hamid SBA (2017) Easy fabrication of highly thermal-stable cellulose nanocrystals using Cr(NO₃)₃ catalytic hydrolysis system: a feasibility study from macro to nano-dimensions. *Materials (Basel)*. <https://doi.org/10.3390/ma10010042>
- Cheng M, Qin Z, Liu Y et al (2014) Efficient extraction of carboxylated spherical cellulose nanocrystals with narrow distribution through hydrolysis of lyocell fibers by using ammonium persulfate as an oxidant. *J Mater Chem A* 2:251–258. <https://doi.org/10.1039/c3ta13653a>
- Chufu A, Yuan H, Zou D et al (2015) Bioresource technology Biomethane production and physicochemical characterization of anaerobically digested teff (*Eragrostis tef*) straw pretreated by sodium hydroxide. *Bioresour Technol* 181:214–219. <https://doi.org/10.1016/j.biortech.2015.01.054>
- Conti ME (2018) Heavy metals in food packagings—the state of the art. *Mineral Components in Foods*. CRC Press, New Jersey, p 339
- Feng Y, Cheng T, Yang W et al (2018) Industrial crops & products characteristics and environmentally friendly extraction of cellulose nano fibrils from sugarcane bagasse. *Ind Crop Prod* 111:285–291. <https://doi.org/10.1016/j.indcrop.2017.10.041>
- Feng Y, Cheng T, Yang W et al (2020) Characterization of cellulose nanocrystals produced by acid-hydrolysis from sugarcane bagasse as agro-waste. *J Mater Phys Chem* 2:1–8
- French AD (2014) Idealized powder diffraction patterns for cellulose polymorphs. *Cellulose* 21:885–896. <https://doi.org/10.1007/s10570-013-0030-4>
- Gichuki J, Kareru PG, Gachanja AN, Ngamau C (2022) Characteristics of microcrystalline cellulose from coir fibers. *J Nat Fibers* 19:915–930. <https://doi.org/10.1080/15440478.2020.1764441>

- Hachaichi A, Kouini B, Kian LK et al (2021) Extraction and characterization of microcrystalline cellulose from date palm fibers using successive chemical treatments. *J Polym Environ* 29:1990–1999. <https://doi.org/10.1007/s10924-020-02012-2>
- Ismail F, Othman NEA, Wahab NA et al (2021) Preparation of microcrystalline cellulose from oil palm empty fruit bunch fibre using steam-assisted acid hydrolysis. *J Adv Res Fluid Mech Therm Sci* 81:88–98. <https://doi.org/10.37934/arfmts.81.1.8898>
- Kamireddy SR, Li J, Tucker M et al (2013) Effects and mechanism of metal chloride salts on pretreatment and enzymatic digestibility of corn stover. *Ind Eng Chem Res* 52:1775–1782. <https://doi.org/10.1021/ie3019609>
- Kapoor M, Panwar D, Kaira GS (2016) Bioprocesses for enzyme production using agro-industrial wastes: technical challenges and commercialization potential. Elsevier, New York, pp 61–93
- Katakajwala R, Mohan SV (2020) Microcrystalline cellulose production from sugarcane bagasse: sustainable process development and life cycle assessment. *J Clean Prod* 249:119342. <https://doi.org/10.1016/j.jclepro.2019.119342>
- Kumar A, Negi YS, Choudhary V, Bhardwaj NK (2014) Characterization of cellulose nanocrystals produced by acid-hydrolysis from sugarcane bagasse as agro-waste. *J Mater Phys Chem* 2:1–8. <https://doi.org/10.12691/jmpc-2-1-1>
- Kürschner KHA (1931) quantitative cellulose bestimmung. *Chemiker Zeitung*, 1931, 55: 161–163. *Zeitschrift Für Pflanzenernährung, Düngung, Bodenkd* 88:1–13
- Le Troedec M, Sedan D, Peyratout C et al (2008) Influence of various chemical treatments on the composition and structure of hemp fibres. *Compos Part A Appl Sci Manuf* 39:514–522. <https://doi.org/10.1016/j.compositesa.2007.12.001>
- Li M, He B, Zhao L (2019) Isolation and characterization of microcrystalline cellulose from cotton stalk waste. *Bio Res* 14:3231–3246. <https://doi.org/10.15376/biores.14.2.3231-3246>
- Lu Q, Tang L, Lin F et al (2014) Preparation and characterization of cellulose nanocrystals via ultrasonication-assisted FeCl₃-catalyzed hydrolysis. *Cellulose* 21:3497–3506. <https://doi.org/10.1007/s10570-014-0376-2>
- Maiti S, Jayaramudu J, Das K et al (2015) Preparation of high crystallinity cellulose nanocrystals (CNCs) by ionic liquid solvolysis. *Biomass Bioenerg* 81:584–591. <https://doi.org/10.1016/j.biombioe.2015.08.016>
- Ohwoavworhwa FO, Mitchell JW, Okhamafe AO (2019) Rice husk as a sustainable source of microcrystalline cellulose: pharmacopoeial, crystalline and spectroscopic characteristics. *Drug Discov* 13:79–87
- Panthapulakkal S, Zereshkian A, Sain M (2006) Preparation and characterization of wheat straw fibers for reinforcing application in injection molded thermoplastic composites. *Bioresour Technol* 97:265–272. <https://doi.org/10.1016/j.biortech.2005.02.043>
- Report R (2011) Heavy metals in packaging Colophon Contact : Segal L, Creely JJ, Martin AE, Conrad CM (1959) An empirical method for estimating the degree of crystallinity of native cellulose using the x-ray diffractometer. *Text Res J* 29:786–794. <https://doi.org/10.1177/004051755902901003>
- Sluiter A, Hames B, Ruiz RO et al (2004) Determination of Structural Carbohydrates and Lignin in Biomass. *Biomass Anal Technol Team Lab Anal Proced* 1617:1–14
- Sluiter A, Hames B, Ruiz R et al (2008) Determination of ash in biomass. NREL laboratory analytical procedure (LAP). *Natl Renew Energy Lab* 18:1–6
- Sluiter A, Ruiz R, Scarlata C et al (2008) Determination of extractives in biomass. *Laborat Analyt Proced* 1617:16
- Sun X, Wu Q, Ren S, Lei T (2015) Comparison of highly transparent all-cellulose nanopaper prepared using sulfuric acid and TEMPO-mediated oxidation methods. *Cellulose* 22:1123–1133. <https://doi.org/10.1007/s10570-015-0574-6>
- Tian D, Chandra RP, Lee JS et al (2017) A comparison of various lignin-extraction methods to enhance the accessibility and ease of enzymatic hydrolysis of the cellulosic component of steam-pretreated poplar. *Biotechnol Biofuels* 10:1–10. <https://doi.org/10.1186/s13068-017-0846-5>
- Trache D, Hussin MH, Hui Chuin CT et al (2016) Microcrystalline cellulose: isolation, characterization and bio-composites application—A review. *Int J Biol Macromol* 93:789–804. <https://doi.org/10.1016/j.ijbiomac.2016.09.056>
- Uddin AH, Khalid RS, Alaama M et al (2016) Comparative study of three digestion methods for elemental analysis in traditional medicine products using atomic absorption spectrometry. *J Anal Sci Technol* 7:1–7. <https://doi.org/10.1186/s40543-016-0085-6>
- Wassie AB, Srivastava VC (2016) Journal of Environmental chemical engineering Teff straw characterization and utilization for chromium removal from wastewater : kinetics, isotherm and thermodynamic modelling. *Biochem Pharmacol* 4:1117–1125. <https://doi.org/10.1016/j.jece.2016.01.019>
- Wassie AB, Srivastava VC (2017) Synthesis and characterization of nano-silica from teff straw. *Int J Nano Res* 46:64–72. <https://doi.org/10.4028/www.scientific.net/JNanoR.46.64>
- Wei H, Donohoe BS, Vinzant TB et al (2011) Elucidating the role of ferrous ion cocatalyst in enhancing dilute acid pretreatment of lignocellulosic biomass. *Biotechnol Biofuels* 4(1):1–16
- Yang S, Zhang Y, Yue W et al (2016) Valorization of lignin and cellulose in acid-steam-exploded corn stover by a moderate alkaline ethanol post-treatment based on an integrated biorefinery concept. *Biotechnol Biofuels* 9:1–14. <https://doi.org/10.1186/s13068-016-0656-1>
- Zhang YHP, Lynd LR (2004) Toward an aggregated understanding of enzymatic hydrolysis of cellulose: Noncomplexed cellulase systems. *Biotechnol Bioeng* 88:797–824. <https://doi.org/10.1002/bit.20282>
- Zhang Y, Li Q, Su J et al (2015) Bioresource Technology A green and efficient technology for the degradation of cellulosic materials : Structure changes and enhanced enzymatic hydrolysis of natural cellulose pretreated by synergistic interaction of mechanical activation and metal salt. *Bioresour Technol* 177:176–181. <https://doi.org/10.1016/j.biortech.2014.11.085>

- Zhang K, Sun P, Liu H et al (2020) Industrial Crops & Products Characterization of nanocellulose extracted from short, medium and long grain rice husks. *Ind Crop Prod* 154:112627. <https://doi.org/10.1016/j.indcrop.2020.112627>
- Zhao T, Chen Z, Lin X et al (2018) Preparation and characterization of microcrystalline cellulose (MCC) from tea waste. *Carbohydr Polym* 184:164–170. <https://doi.org/10.1016/j.carbpol.2017.12.024>
- Zhuang J, Li M, Pu Y et al (2020) Observation of potential contaminants in processed biomass using fourier transform infrared spectroscopy. *Appl Sci* 10:1–13. <https://doi.org/10.3390/app10124345>

Publisher's Note Springer Nature remains neutral with regard to jurisdictional claims in published maps and institutional affiliations.

Springer Nature or its licensor (e.g. a society or other partner) holds exclusive rights to this article under a publishing agreement with the author(s) or other rightsholder(s); author self-archiving of the accepted manuscript version of this article is solely governed by the terms of such publishing agreement and applicable law.